

# Elastic properties and electronic structures of antiperovskite-type $\text{InNCo}_3$ and $\text{InNNi}_3$

Z. F. Hou

*Department of Physics, Fudan University, Shanghai, 200433, P. R. China*

## Abstract

We have performed the first-principles calculations to study the elasticity, electronic structure, and magnetism of  $\text{InNCo}_3$  and  $\text{InNNi}_3$ . The independent elastic constants are derived from the second derivative of total energy as a function of strain, and the elastic modulus are predicted according to the Voigt-Reuss-Hill approximation. Our calculations show that the bulk modulus of  $\text{InNCo}_3$  is slightly larger than that of  $\text{InNNi}_3$  due to a smaller lattice constant for  $\text{InNCo}_3$ . For  $\text{InNCo}_3$  the ferromagnetic state is energetically preferable to the paramagnetic state, while the ground state of  $\text{InNNi}_3$  is a stable paramagnetic (non-magnetic) state. This is due to the different strength of  $2p$ - $3d$  hybridization for the N-Co and N-Ni atoms in  $\text{InNCo}_3$  and  $\text{InNNi}_3$ .

## I. INTRODUCTION

The ternary nitrides or carbides with the general formula  $AXM_3$  (A: divalent or trivalent element; X: carbon or nitrogen; and M: transition metal) are already known for several decades<sup>1-3</sup>. These compounds crystalize in a cubic anti-perovskite structure (A: cube-corner position; X: body-center position; M: face-center position) and exhibit a wide range of interesting physical properties<sup>1</sup>, such as giant magneto-resistance<sup>4</sup> and nearly zero temperature coefficient resistivity<sup>5</sup>. They have renewedly attracted considerable attention due to the discovery of superconductivity at  $\sim 8$  K in intermetallic compound  $MgCNi_3$ <sup>6</sup>.

Considering the Ni-rich composition, it is expected that the ferromagnetism could exist in  $MgCNi_3$ . However, the absence of ferromagnetism was observed in experiment<sup>6</sup> for  $MgCNi_3$ . From the electronic structures obtained by the first-principles calculations<sup>7-10</sup>, the non-ferromagnetic ground state of  $MgCNi_3$  is ascribed to a reduced Stoner factor that results from a strong hybridization between the Ni-3*d* and C-2*p* electrons. For other Ni-based ternary carbides  $ACNi_3$  (e.g., A = Al, Ca, In, Zn, and Cd), the first-principles calculations<sup>10-14</sup> also show that the ground states of these compounds are non-magnetic and the C-Ni bonding exhibits nearly same characteristics as the one in  $MgCNi_3$ . Therefore, this indicates that the change of composition A could not induce the ferromagnetism in  $ACNi_3$ . On the other side, it raises a question whether the change of composition X or M can lead to the appearance of ferromagnetism in  $AXM_3$  or not.

Very recently, the antiperovskite-type compounds  $InN_yCo_3$  and  $InN_yNi_3$  ( $y \sim 1.0$  and  $0.8$ , respectively) have been synthesized by solid-gas reactions of metal powders with  $NH_3$  and they have been reported to have spin-glass-like properties based on the measurements of temperature dependence magnetization.<sup>15</sup> The recent first-principles calculations<sup>12</sup> showed that the non-stoichiometry could affect the magnetic properties of  $ACNi_3$  (e.g.,  $AlCNi_3$  and  $GaCNi_3$ ) and suggested that the tendencies toward magnetism found in experiments<sup>16-19</sup> for these compounds should be explained by the deviation of the Ni/C atomic ratio from the ideal stoichiometry. To shed more light on the understanding on the magnetic properties of  $InNCo_3$  and  $InNNi_3$  reported in experiment<sup>15</sup>, it is of great importance to theoretically study the electronic structures of these two compounds as well as the nature of the N-Co and N-Ni bondings.

In order to completely understand the electronic structures and magnetic ground states of

InNiCo<sub>3</sub> and InNiNi<sub>3</sub> with cubic anti-perovskite structure, we carried out the first-principles calculations on these compounds using the pseudopotentials method with plane-wave basis set within the local density approximation and the generalized gradient approximation. Since the elastic properties of a solid are highly associated with various fundamental solid-state properties such as phonon spectra, specific heat, Debye temperature, and so on, we have calculated the independent elastic constant and the elastic moduli of InNiCo<sub>3</sub> and InNiNi<sub>3</sub>.

## II. COMPUTATIONAL DETAILS

All calculations on antiperovskite-type InNiCo<sub>3</sub> and InNiNi<sub>3</sub> were performed using the Quantum ESPRESSO code<sup>20</sup>, which is based on the density functional theory (DFT)<sup>21</sup>. The electronic exchange-correlation potential was calculated within the local density approximation (LDA)<sup>22,23</sup> and the generalized gradient approximation using the scheme of Perdew-Burke-Ernzerhof (PBE)<sup>24</sup>. The spin polarization was also considered in the calculation in order to assess the magnetic properties of these compounds. Electron-ion interaction was represented by the norm-conserving optimized<sup>25</sup> designed nonlocal pseudopotentials. The 4*d* electrons are explicitly included in the valence of In. The electronic wavefunctions were expanded by the plane waves up to a kinetic energy cutoff of 55 Ry. The **k**-point sampling in Brillouin zone (BZ) of simple cubic lattice was treated with the Monkhorst-Pack scheme<sup>26</sup> and a 20×20×20 **k**-point mesh (i.e., 286 irreducible points in the first BZ) was used. The chosen plane-wave cutoff and number of **k** points were carefully checked to ensure that the total energy was converged to be better than 1 mRy/cell. The total energies are obtained as a function of volume and they are fitted with the Birch-Murnaghan 3rd-order equation of states (EoS)<sup>27</sup> to give the equilibrium lattice constant and other ground state properties. During the calculation of density of states (DOS), a dense **k**-point mesh of 30×30×30 is used, the total DOS is computed by the tetrahedron method<sup>28</sup>, and the atomic-projected DOS is calculated by the Löwdin populations<sup>29</sup>.

For a cubic crystal, its independent elastic constants are  $c_{11}$ ,  $c_{12}$ , and  $c_{44}$ . To determine the elastic constants of InNiCo<sub>3</sub> and InNiNi<sub>3</sub> by means of the curvature of the internal energy versus the strain curves<sup>30,31</sup>, three strain modes<sup>32</sup> are adopted and their nonzero strains are as follows: (1)  $\epsilon_{11} = \epsilon_{22} = \delta$ ,  $\epsilon_{33} = (1 + \delta)^{-2} - 1$ ; (2)  $\epsilon_{11} = \epsilon_{22} = \epsilon_{33} = \delta$ ; and (3)  $\epsilon_{12} = \epsilon_{21} = \delta/2$ ,  $\epsilon_{33} = \delta^2/(4 - \delta^2)$ . The deformation magnitudes  $\delta$  from -0.012 to 0.012

in the step of 0.03 are applied in the first and second strain modes, and  $\delta$  from -0.04 to 0.04 in the step 0.01 are adopted in the third strain mode. Once the independent elastic constants for single crystal properties are obtained through the above procedure, the elastic moduli (e.g., the shear modulus and the bulk modulus) of polycrystalline aggregates can be estimated according to the Voigt-Reuss-Hill approximation<sup>33-35</sup>. In the Voigt average<sup>33</sup>, the shear modulus and the bulk modulus of cubic lattice are given by

$$G_V = \frac{1}{5} [(c_{11} - c_{12}) + 3c_{44}] \quad (1)$$

and

$$B_V = \frac{1}{3}(c_{11} + 2c_{12}), \quad (2)$$

while in the Reuss average<sup>34</sup> they are given by

$$G_R = \frac{5}{4(s_{11} - s_{12}) + 3s_{44}} \quad (3)$$

and

$$B_R = \frac{1}{3s_{11} + 6s_{12}} \quad (4)$$

with the relations  $c_{44} = s_{44}^{-1}$ ,  $c_{11} - c_{12} = (s_{11} - s_{12})^{-1}$ , and  $c_{11} + 2c_{12} = (s_{11} + 2s_{12})^{-1}$  in the cubic lattice, where  $s_{ij}$  are the elastic compliance constants. Therefore,  $G_R$  and  $B_R$  in the cubic lattice can be rewritten as

$$G_R = \left[ \frac{4}{5}(c_{11} - c_{12})^{-1} + \frac{3}{5}c_{44}^{-1} \right]^{-1}, \quad (5)$$

and

$$\begin{aligned} B_R &= \frac{1}{3} [(c_{11} + 2c_{12})] \\ &= B_V. \end{aligned} \quad (6)$$

In the Hill empirical average<sup>35</sup>, the shear modulus and the bulk modulus are taken as  $G = \frac{1}{2}(G_V + G_R)$  and  $B = \frac{1}{2}(B_V + B_R)$ , respectively. Knowing  $G$  and  $B$ , the Young's modulus  $E$  and Poisson's ratio  $\nu$ , which are frequently measured for polycrystalline materials when investigating their hardness, can be calculated from the isotropic relations:

$$E = \frac{9BG}{3B + G} \quad (7)$$

and

$$\nu = \frac{3B - 2G}{2(3B + G)}. \quad (8)$$

### III. RESULTS AND DISCUSSIONS

#### A. Structural properties

In experiment with the powder X-ray diffraction patterns, Cao et al<sup>15</sup> have reported that  $\text{InN}_y\text{Co}_3$  and  $\text{InN}_y\text{Ni}_3$  ( $y \sim 1.0$  and  $0.8$ , respectively) have the cubic anti-perovskite structure with the space group  $221(Pm\bar{3}m)$  and the corresponding lattice parameters were  $3.854 \text{ \AA}$  and  $3.844 \text{ \AA}$ , respectively. Starting from the experimental data, we have calculated the total energies of unit cell at a series of volumes for each compound in the paramagnetic (PM) and ferromagnetic (FM) states. The results are presented in Fig. 1. It is found that the energy difference between the FM and PM states is  $-0.0397 \text{ eV}$  ( $-0.226 \text{ eV}$ ) in the LDA (GGA) calculations for  $\text{InNCo}_3$  and  $0.0 \text{ eV}$  for  $\text{InNNi}_3$ . The total magnetic moment of  $\text{InNCo}_3$  is about  $2.14 \mu_B$  ( $2.91 \mu_B$ ) and the local magnetic moment of each In ion is about  $0.69 \mu_B$  ( $0.94 \mu_B$ ) in LDA (GGA) calculations. The total magnetic moment of  $\text{InNNi}_3$  and the local magnetic moment of each Ni atom are zero. These indicate that the ferromagnetic state is energetically favorable to  $\text{InNCo}_3$  and the ground state of  $\text{InNNi}_3$  is paramagnetic state (non-magnetic). The obtained equilibrium lattice constant ( $a_0$ ), bulk modulus ( $B$ ), and first pressure derivative of bulk modulus ( $B'$ ) of  $\text{InNCo}_3$  and  $\text{InNNi}_3$  are listed in Table I. In our calculations, the predicted lattice constant of  $\text{InNCo}_3$  is slightly larger than that of  $\text{InNNi}_3$ , which is opposite to the trend reported in experiment<sup>15</sup>. This may be due to the deviation of the Ni/N atomic ratio from the ideal stoichiometry in experiment for  $\text{InN}_y\text{Ni}_3$ . In addition, it can be seen that the deviations of the LDA (GGA) lattice constants of both the  $\text{InNCo}_3$  and  $\text{InNNi}_3$  with respect to the experimental values are less than 2.6% (1.0%). That is to say, the calculated equilibrium lattice constants of  $\text{InNCo}_3$  and  $\text{InNNi}_3$  are in excellent agreement with the experimental data<sup>15</sup>.

#### B. Elastic properties

The calculated independent elastic constants for single crystal of  $\text{InNCo}_3$  and  $\text{InNNi}_3$  are listed in Table II. Based on the Voigt-Reuss-Hill approximation<sup>33-35</sup>, the elastic moduli of  $\text{InNCo}_3$  and  $\text{InNNi}_3$  are estimated and the results are listed in Table II. For the bulk moduli of  $\text{InNCo}_3$  and  $\text{InNNi}_3$ , the estimations based on the independent elastic constants agree well those obtained by the fit of the Birch-Murnaghan 3rd-order EoS. To the best of

our knowledge, no experimental data or theoretical results for the elasticity of  $\text{InNC}_3$  and  $\text{InNNi}_3$  compounds have been reported up to now. Considering that the elastic properties of  $\text{ZnNNi}_3$ ,  $\text{InNSc}_3$ , and  $\text{InCNi}_3$  with cubic anti-perovskite structure have been studied recently and the theoretical results are available in literature<sup>14,36–38</sup>, it will be meaningful to compare them with those of  $\text{InNC}_3$  and  $\text{InNNi}_3$  compounds. The order of bulk moduli of these five compounds from low to high is:  $B(\text{InNSc}_3) < B(\text{InNNi}_3) < B(\text{InCNi}_3) < B(\text{InNC}_3) < B(\text{ZnNNi}_3)$ . This could be understood from the trend in lattice constants ( $a$ ) of these compounds (i.e.,  $a(\text{InNSc}_3) > a(\text{InNNi}_3) > a(\text{InCNi}_3) > a(\text{InNC}_3) > a(\text{ZnNNi}_3)$ ) as well as the relationship between bulk modulus and equilibrium volume (i.e.,  $B \sim V^{-1}$ )<sup>39</sup>. The GGA lattice constants of  $\text{InNSc}_3$ ,  $\text{ZnNNi}_3$ , and  $\text{InCNi}_3$  are 4.411 Å<sup>36</sup>, 3.77 Å<sup>37</sup>, and 3.880 Å<sup>14</sup>, respectively. The order of shear modulus from low to high is:  $G(\text{ZnNNi}_3 \text{ and } \text{InNNi}_3) < G(\text{InCNi}_3) < G(\text{InNC}_3)$ . Pugh<sup>40</sup> has proposed that a high  $B/G$  ratio may be associated with better ductility whereas a low value would correspond to a more brittleness, and the critical value separating ductile and brittle materials is around 1.75. From the results of  $B/G$  ratio for  $\text{InNC}_3$ ,  $\text{InNNi}_3$ ,  $\text{InNSc}_3$ ,  $\text{ZnNNi}_3$ , and  $\text{InCNi}_3$ , it is found that only  $\text{InNSc}_3$  can be classified as brittle materials and others may be ductile materials. Furthermore,  $\text{InNNi}_3$  seems to be more ductile than  $\text{InNC}_3$ .

For a cubic crystal, its mechanical stability requires that its three independent elastic constants should satisfy the following relations<sup>41</sup>:

$$(c_{11} - c_{12}) > 0, c_{11} > 0, c_{44} > 0, (c_{11} + 2c_{12}) > 0. \quad (9)$$

These conditions also lead to a restriction on the magnitude of  $B$ :

$$c_{12} < B < c_{11}. \quad (10)$$

The predicted  $c_{ij}$  values (see Table II) for  $\text{InNC}_3$  and  $\text{InNNi}_3$  satisfy these conditions, indicating that cubic antiperovskite-type compounds  $\text{InNC}_3$  and  $\text{InNNi}_3$  are mechanically stable.

### C. Electronic structures

In order to understand the different magnetic ground states for  $\text{InNC}_3$  and  $\text{InNNi}_3$ , we examined the electronic structures of these two compounds. For the simplicity in discussion,

only the GGA results are presented below. The calculated electronic band structures along the high symmetry directions in the Brillouin zone are shown in Fig. 2. As discussed above, for  $\text{InNCo}_3$  the ferromagnetic state is energetically preferable to the paramagnetic state, and hence it is clearly seen that the spin-splitting occurs in the bands around the  $E_F$ . For  $\text{InNCo}_3$  the profile of majority spin bands looks roughly similar to the one of minority spin bands, however only one band in the majority spin bands crosses the Fermi level and the corresponding band with same dispersion in the minority spin bands is unoccupied. In addition, two bands in the minority spin bands across the Fermi level of  $\text{InNCo}_3$  (see Fig. 2(a)). For  $\text{InNNi}_3$  the ferromagnetic state is not energetically preferable to the paramagnetic state, consequently, the majority and minority spin bands are degenerated, that is to say, no spin-splitting occurs in the band structure (see Fig. 2(b)). It is interesting to note that the whole feature of majority spin bands of  $\text{InNNi}_3$  is very similar to the one of  $\text{InNCo}_3$ . In order to reveal the detailed character of band structure, the total density of states (DOS) and the angular-momentum-projected DOS of each atom in  $\text{InNCo}_3$  and  $\text{InNNi}_3$  are presented in Fig. 3. For both  $\text{InNCo}_3$  and  $\text{InNNi}_3$ , the four bands from -9 eV to -5 eV come mainly from the N  $2p$  states and In  $5s$  states, and the five bands roughly from -5 eV to -2.5 eV have significant contribution from  $3d-t_{2g}$  states of transition metal atoms (Co/Ni) and the  $5p$  state of In atom. For the bands from -2.5 eV to 0 eV (i.e., the Fermi level), they are dominated by the  $3d$  states of transition metal atoms (Co/Ni) and have small contribution from the  $2p$  states of N atom. Because the number of  $3d$  electrons in Co is one less than that of Ni, two minority spin bands composed of the  $3d-t_{2g}$  states around the Fermi level are unoccupied in  $\text{InNCo}_3$ , while the counterpart in the  $\text{InNNi}_3$  are occupied. This also results in different behavior of spin-splitting in  $\text{InNCo}_3$  and  $\text{InNNi}_3$ . Due to the significant spin-splitting around the Fermi level in  $\text{InNCo}_3$ , the hybridization between the Co  $3d$  and N  $2p$  states in  $\text{InNCo}_3$  are slightly weaker than the one between Ni  $3d$  and N  $2p$  states in  $\text{InNNi}_3$ (see Fig. 3).

The contributions of each kind of atoms to the DOS at the  $E_F$  of  $\text{InNCo}_3$  and  $\text{InNNi}_3$  are listed in Table III. The total DOS at the  $E_F$  of  $\text{InNCo}_3$  is about 2.761 states/eV per formula unit (f.u.) in the GGA calculations, which is larger than that of  $\text{InNNi}_3$ , and its main contribution comes from Co  $3d$  states which accounts for 87%. For  $\text{InNNi}_3$  in the GGA calculations, the contribution of Ni  $3d$  states to the the total DOS at the  $E_F$  (i.e., 1.803 states/eV.f.u.) accounts for 72%. These indicate the  $3d$  states of transition metal atoms in

InNCo<sub>3</sub> and InNNi<sub>3</sub> play dominant roles in the total density of states of these compounds.

In order to understand the bonding nature among the ions in InNCo<sub>3</sub> and InNNi<sub>3</sub>, we analyzed the charge density contours of InNCo<sub>3</sub> and InNNi<sub>3</sub> in the(110) plane, as shown in Fig. 4. From Fig. 4, it is found that a certain amount of charges are accumulated in the intermediate region between N and Co atoms in InNCo<sub>3</sub>, and slightly more charges are accumulated in the intermediate region between N and Ni atoms in InNNi<sub>3</sub>. This gives an evidence for the strong hybridization between N and transition metal (Co/Ni) atoms, indicating that the N-Co and N-Ni bondings exhibit strong covalent characteristics and the latter is slightly stronger than the former. The similar bonding characteristics for Ni-N atoms or Ni-C atoms were also found in other Ni-based ternary nitrides or carbides AXNi<sub>3</sub><sup>10,14,37,38</sup>. Therefore, our results suggest that the magnetic properties of InNNi<sub>3</sub> reported in experiment<sup>15</sup> are very likely due to the non-stoichiometry effect, which was also found in the cases of AlCNi<sub>3</sub> and GaCNi<sub>3</sub><sup>12,16-19</sup>.

#### IV. CONCLUSIONS

In summary, we performed the first-principles calculations to study the elastic and electronic properties of cubic antiperovskites InNCo<sub>3</sub> and InNNi<sub>3</sub>. Based on the Voigt, Reuss and Hill bounds, the shear, Young's moduli and Poisson's ratio have also been estimated for the InNCo<sub>3</sub> and InNNi<sub>3</sub> polycrystals. The theoretically predicted equilibrium lattice parameters are in good agreement with the available experimental data. Our calculations show that the 3*d* states of transition metal atoms in InNCo<sub>3</sub> and InNNi<sub>3</sub> play dominant roles near the Fermi levels. InNCo<sub>3</sub> energetically prefers to the ferromagnetic state. The magnetic ground state of InNNi<sub>3</sub>, which is same to other Ni-based ternary nitrides or carbides with a cubic anti-perovskite structure, is a stable paramagnetic (non-magnetic) state. This could be understood from that the hybridization between Ni-3*d* and N-2*p* states in InNNi<sub>3</sub> is slightly stronger than the one between Co-3*d* and N-2*p* states in InNCo<sub>3</sub> because of the more 3*d* electrons in Ni.



## Acknowledgments

The author acknowledges support from National Natural Science Foundation of China under Grant No. 10674028.

---

- <sup>1</sup> J. B. Goodenough, J. M. Longo, Magnetic and other properties of oxides and related compounds, in: K.-H. Hellwege, O. Madelung (Eds.), Landolt-Bornstein, New Series, Group III, Vol. 4a, Springer-Verlag, Berlin, 1970.
- <sup>2</sup> M. Y. Chern, D. A. Vennos, F. J. DiSalvo, *J. Solid State Chem.* 96 (1992) 415.
- <sup>3</sup> J. Jäger, D. Stahl, P. C. Schmidt, R. Kniep, *Angew. Chem.* 105 (1993) 738.
- <sup>4</sup> W. S. Kim, E. O. Chi, J. C. Kim, H. S. Choi, N. H. Hur, *Solid State Commun.* 119 (2001) 507.
- <sup>5</sup> E. O. Chi, W. S. Kim, N. H. Hur, *Solid State Commun.* 120 (2001) 307.
- <sup>6</sup> T. He, Q. Huang, A. P. Ramirez, Y. Wang, K. A. Regan, N. Rogado, M. A. Hayward, M. K. Haas, J. S. Slusky, K. Inumara, H. W. Zandbergen, N. P. Ong, R. J. Cava, *Nature* 411 (2001) 54.
- <sup>7</sup> D. J. Singh, I. I. Mazin, *Phys. Rev. B* 64 (2001) 140507.
- <sup>8</sup> J. H. Shim, S. K. Keson, B. I. Min, *Phys. Rev. B* 64 (2001) 180510.
- <sup>9</sup> H. Rosner, R. Weht, M. D. Johannes, W. E. Pickett, E. Tosatti, *Phys. Rev. Lett.* 88 (2002) 027001.
- <sup>10</sup> S. Q. Wu, Z. F. Hou, Z. Z. Zhu, *Solid State Sci.* 11 (2009) 251.
- <sup>11</sup> C. M. I. Okoye, *Solid State Commun.* 136 (2005) 605.
- <sup>12</sup> M. Sieberer, P. Mohn, J. Redinger, *Phys. Rev. Lett.* 75 (2007) 024431.
- <sup>13</sup> G. H. Zhong, J. L. Wang, Z. Zeng, X. H. Zheng, H. Q. Lin, *J. Appl. Phys.* 101 (2007) 09G520.
- <sup>14</sup> S. Q. Wu, Z. F. Hou, Z. Z. Zhu, *Physica B* 403 (2008) 4232.
- <sup>15</sup> W. H. Cao, B. He, C. Z. Liao, L. H. Yang, L. M. Zeng, C. Dong, *J. Solid State Chem.* 182 (2009) 3353.
- <sup>16</sup> A. F. Dong, G. C. Che, W. W. Huang, S. L. Jia, H. Chen, Z. X. Zhao, *Physica C* 422 (2005) 65.
- <sup>17</sup> P. Tong, Y. P. Sun, X. B. Zhu, W. H. Song, *Phys. Rev. B* 74 (2006) 22441.
- <sup>18</sup> P. Tong, Y. P. Sun, X. B. Zhu, W. H. Song, *Phys. Rev. B* 73 (2006) 245106.

- <sup>19</sup> P. Tong, Y. Sun, X. Zhu, W. Song, *Solid State Commun.* 141 (2007) 336.
- <sup>20</sup> S. Baroni, A. D. Corso, S. de Gironcoli, P. Giannozzi, C. Cavazzoni, G. Ballabio, S. Scandolo, G. Chiarotti, P. Focher, A. Pasquarello, K. Laasonen, A. Trave, R. Car, N. Marzari, A. Kokalj, <http://www.pwscf.org/>.
- <sup>21</sup> W. Kohn, L. J. Sham, *Phys. Rev.* 140 (1965) A1133.
- <sup>22</sup> D. M. Ceperley, B. J. Alder, *Phys. Rev. Lett.* 45 (1980) 566.
- <sup>23</sup> J. P. Perdew, A. Zunger, *Phys. Rev. B* 23 (1981) 5048.
- <sup>24</sup> J. P. Perdew, K. Burke, M. Ernzerhof, *Phys. Rev. Lett.* 77 (1996) 3865.
- <sup>25</sup> A. M. Rappe, K. M. Rabe, E. Kaxiras, J. D. Joannopoulos, *Phys. Rev. B* 41 (1990) 1227.
- <sup>26</sup> H. J. Monkhorst, J. D. Pack, *Phys. Rev. B* 13 (1976) 5188.
- <sup>27</sup> F. Birch, *Phys. Rev.* 71 (1947) 809.
- <sup>28</sup> G. Lehmann, M. Taut, *Phys. Stat. Sol. (b)* 54 (1972) 469.
- <sup>29</sup> D. Sanchez-Portal, E. Artacho, J. M. Soler, *Solid State Commun.* 95 (1995) 685.
- <sup>30</sup> M. J. Mehl, *Phys. Rev. B* 47 (1993) 2493.
- <sup>31</sup> S. Q. Wu, Z. F. Hou, Z. Zhu, *Solid State Commun.* 143 (2007) 425.
- <sup>32</sup> Z. F. Hou, *Solid State Sci.* 10 (2008) 1651.
- <sup>33</sup> D. W. Voigt, *Lehrbuch der Kristallphysik*, Taubner, Leipzig, 1928.
- <sup>34</sup> A. Reuss, *Z. Angew. Math. Mech* 9 (1929) 55.
- <sup>35</sup> R. Hill, *Proc. Phys. Soc. London A* 65 (1952) 349.
- <sup>36</sup> M. Mattesini, M. Magnuson, F. Tasnádi, C. Höglund, I. A. Abrikosov, L. Hultman, *Phys. Rev. B* 79 (2009) 125122.
- <sup>37</sup> C. Li, W. G. Chen, F. Wang, S. F. Li, Q. Sun, S. Wang, Y. Jia, *J. Appl. Phys.* 105 (2009) 123921.
- <sup>38</sup> I. R. Shein, V. V. Bannikov, A. L. Ivanovskii, *Phys. Stat. Sol. (b)* 247 (2010) 72.
- <sup>39</sup> M. L. Cohen, *Phys. Rev. B* 32 (1985) 7988.
- <sup>40</sup> S. F. Pugh, *Philos. Mag.* 45 (1954) 823.
- <sup>41</sup> D. C. Wallace, *Thermodynamics of Crystals*, Wiley, New York, 1972.

TABLE I: Calculated lattice constants ( $a$ , in Å), bulk modulus ( $B$ , in GPa), and the first pressure derivative  $B'$  of bulk modulus for  $\text{InNC}_3$  and  $\text{InNNi}_3$ .  $\Delta E_{\text{tot}}^{\text{FM-PM}}$  (in eV per formula unit) is the difference between the total energies of ferromagnetic (FM) and paramagnetic (PM) states for  $\text{InNC}_3$  and  $\text{InNNi}_3$ . The available experimental values are also listed.

	InNC <sub>3</sub>					InNNi <sub>3</sub>		
	LDA		GGA		Expt. <sup>15</sup>	LDA	GGA	Expt. <sup>15</sup>
	PM	FM	PM	FM		PM/FM	PM/FM	
$a$	3.744	3.753	3.835	3.855	3.8541	3.784	3.882	3.8445
$B$	255.78	243.06	211.29	194.17		226.91	179.93	
$B'$	4.497	4.483	5.570	5.568		4.761	4.281	
$\Delta E_{\text{tot}}^{\text{FM-PM}}$	-	-0.0397	-	-0.226		0.0	0.0	

TABLE II: Calculated elastic constants ( $c_{11}$ ,  $c_{12}$ , and  $c_{44}$ , in GPa), shear modulus ( $G$ , in GPa), Young's modulus ( $E$ , in GPa), and Poisson's ratio ( $\nu$ ) of  $\text{InNCo}_3$  and  $\text{InNNi}_3$ . The Voigt shear modulus ( $G_V$ , in GPa) and the Reuss shear modulus ( $G_R$ , in GPa) are also presented. For comparison, the elastic properties of  $\text{InNSc}_3$ ,  $\text{ZnNNi}_3$ , and  $\text{InCNi}_3$  compounds with a cubic anti-perovskite structure are listed.

Compound	Method	$c_{11}$	$c_{12}$	$c_{44}$	$G_V$	$G_R$	$B$	$G$	$E$	$\nu$	$B/G$
$\text{InNCo}_3$	LDA	389.11	171.12	102.55	105.13	105.03	243.78	105.08	275.63	0.311	2.320
	GGA	317.54	126.76	94.98	95.14	95.14	190.35	95.14	224.67	0.286	2.001
$\text{InNNi}_3$	LDA	356.77	164.23	69.06	80.35	78.12	228.41	79.24	212.94	0.344	2.895
	GGA	274.08	131.20	60.01	64.58	64.11	178.83	64.35	172.37	0.339	2.779
$\text{InNSc}_3$	GGA <sup>36</sup>	238.57	54.28	90.76	91.31	91.31	115.71	91.31	216.88	0.188	1.267
$\text{ZnNNi}_3$	GGA <sup>37</sup>	354.28	134.01	48.06	72.89	62.05	207.43	67.47	182.61	0.353	3.074
	GGA <sup>38</sup>	364.20	124.90	32.69	67.47	46.09	204.67	56.78	155.92	0.373	3.604
$\text{InCNi}_3$	LDA <sup>14</sup>	414.67	135.72	68.02	96.60	85.56	228.71	91.08	241.22	0.324	2.511
	GGA <sup>14</sup>	344.20	106.30	62.68	85.19	77.31	185.60	81.25	212.70	0.309	2.284

TABLE III: Total and partial density of states at the Fermi level ( $N(E_F)$ , in states/eV.f.u.) for  $\text{InNC}_3$  and  $\text{InNNi}_3$ .

		Total density of states	Partial density of states		
			In	N	$\text{Co}_3/\text{Ni}_3$
$\text{InNC}_3$	LDA	3.811	0.073	0.337	3.401
	GGA	2.761	0.144	0.169	2.448
$\text{InNNi}_3$	LDA	1.580	0.160	0.212	1.208
	GGA	1.803	0.180	0.256	1.367

## Figure Captions

- FIG. 1: Total energy (in eV per formula unit) versus the atomic volume (in  $\text{\AA}^3$ ) for  $\text{InNC}_3$  (upper panel)  $\text{InNNi}_3$  (lower panel).
- FIG. 2: (Color online) Electronic band structures obtained with GGA for the majority (red solid line) and minority (blue dashed line) spins of (a)  $\text{InNC}_3$  and (b)  $\text{InNNi}_3$ .
- FIG. 3: Total and partial density of states (DOS) of  $\text{InNC}_3$  (left panel) and  $\text{InNNi}_3$  (right panel) obtained with the spin-polarized GGA calculations.
- FIG. 4: Charge density contours of the (110) plane for (a)  $\text{InNC}_3$  and (b)  $\text{InNNi}_3$  obtained with the spin-polarized GGA calculations.

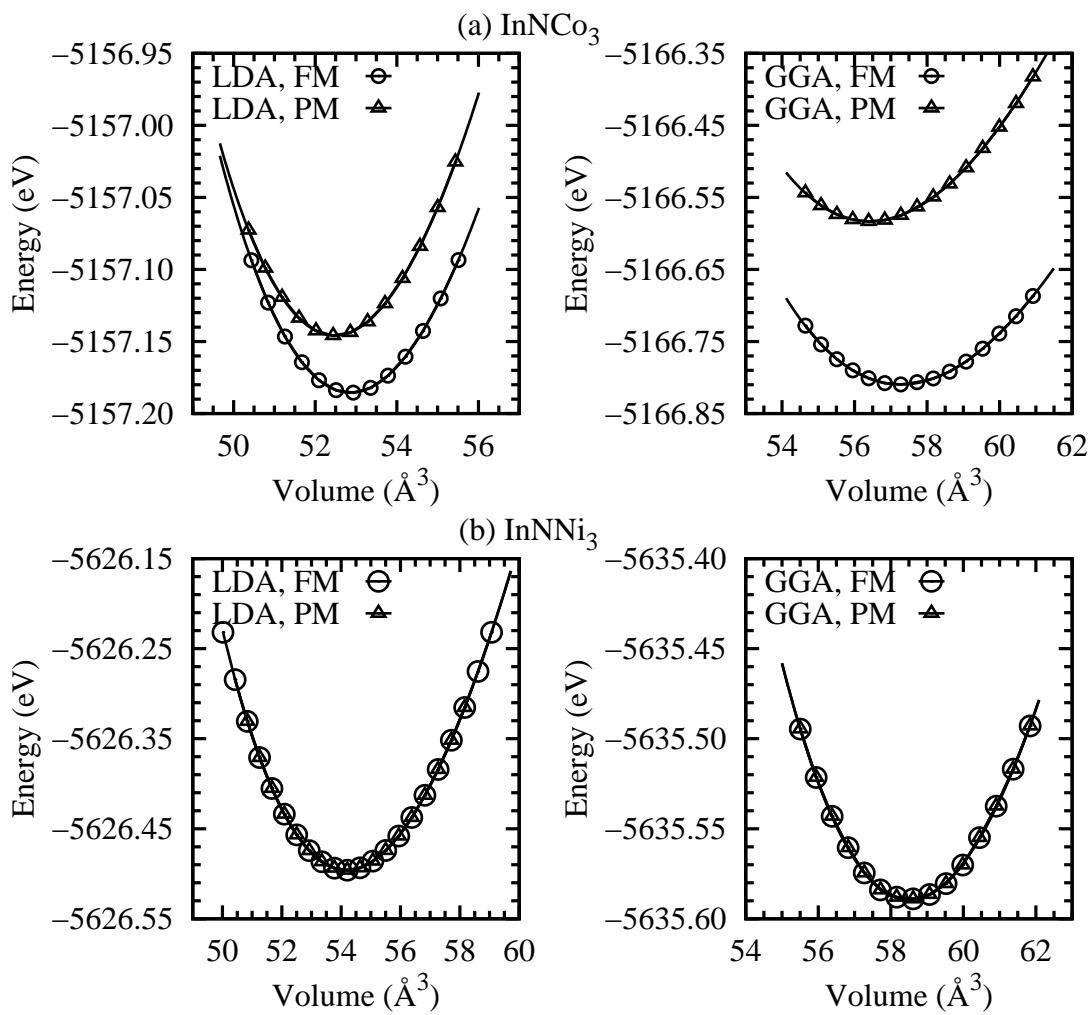


FIG. 1:

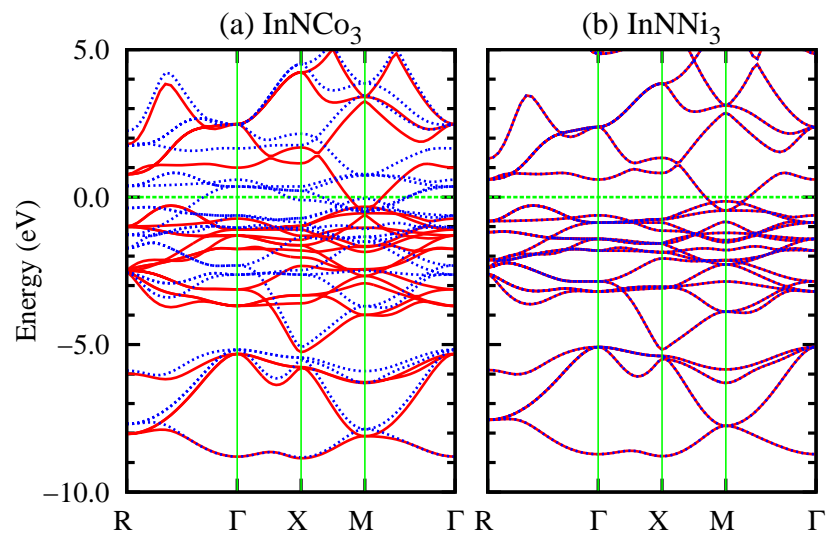


FIG. 2:



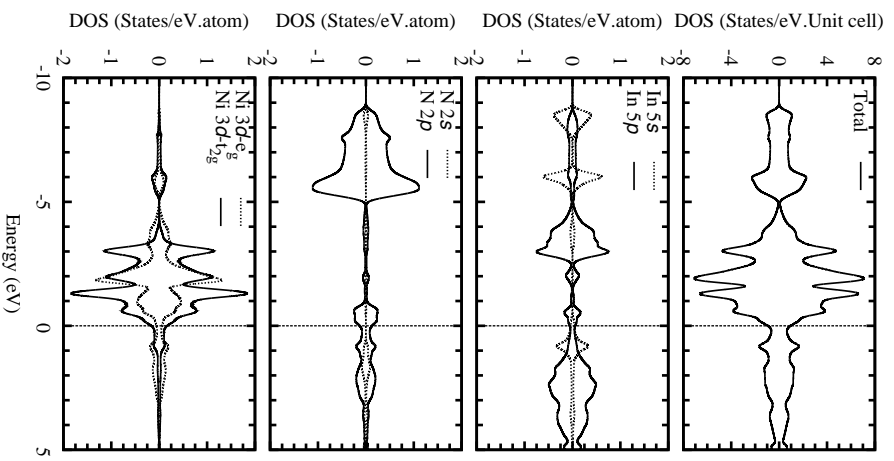
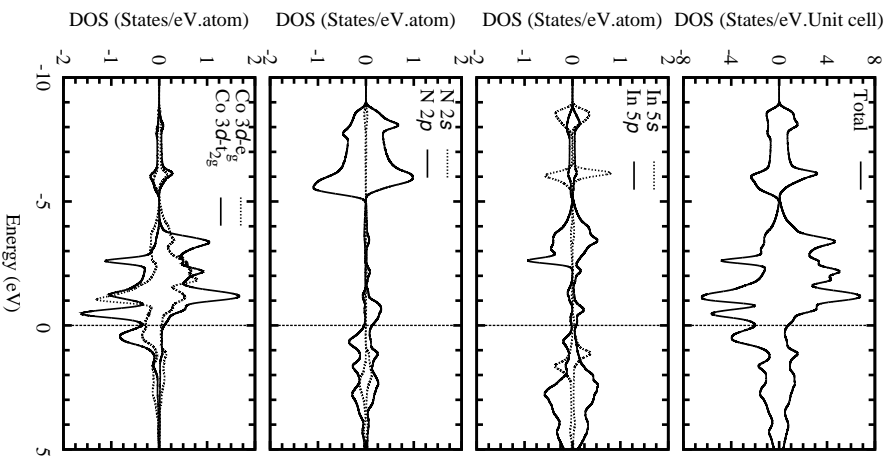


FIG. 3:

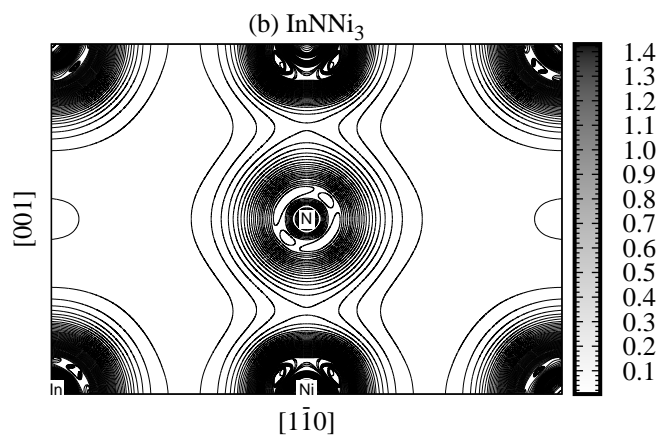
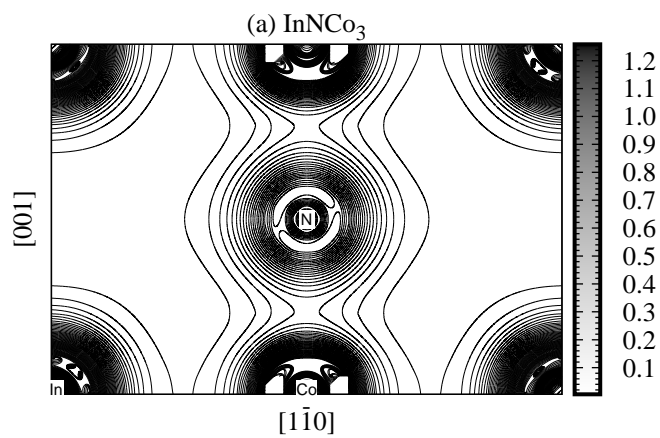


FIG. 4: